RESEARCH

Solid self-nanoemulsifying drug delivery systems of nimodipine: development and evaluation

Mohit Kumar[1], Pooja A. Chawla[2]* , Abdul Faruk[1]* and Viney Chawla[2]*

Abstract

Background This study aimed to formulate solid self-nanoemulsifying drug delivery systems (SNEDDS) for nimodipine (NIM). The selection of Cremophor RH 40, Lipoxol 300, and PEG 400 as oil, surfactant, and co-surfactant was based on solubility and self-emulsification assessments. A ternary phase diagram determined the optimal oil to Smix (surfactant/co-surfactant) ratio (40:60). By utilizing liquid SNEDDS (NIM-SNEDDS) as an adsorbate and chitosan EDTA microparticles, developed through spray drying (SD-CHEM) and solvent evaporation (SE-CHEM) as adsorbents, the solid SNEDDS were created (NIM-SD-SSNEDDS and NIM-SE-SSNEDDS, respectively).

Results Both solid formulations exhibited favourable drug loading (NIM-SD-SSNEDDS = 79.67 ± 2.97%, NIM-SE-SSNEDDS = 77.76 ± 4.29%), excellent flowability, and drug amorphization as per XRD and DSC analysis. Scanning electron microscopy revealed smoothening and filling of adsorbent surfaces by adsorbate (with size range NIM-SD-SSNEDDS = 10–15 μm, NIM-SE-SSNEDDS = 20–25 μm). FTIR confirmed no interaction of drug and excipients. Stability studies demonstrated the physical and thermodynamic stability of reconstituted nanoemulsions with droplet size, PDI, zeta potential, emulsification time, % transmittance and cloud temperature for NIM-SD-SSNEDDS as 247.1 nm, PDI 0.620, 1.353 mV, 38–41 s, 94.64%, 54 °C and for NIM-SE-SSNEDDS as 399.6 nm, PDI 0.821, 1.351 mV, 40–48 s, 92.96%, 49 °C, respectively. FE-SEM images showed globules formed with small sizes, and there was no coalescence evidence, implying the reconstituted nanoemulsions' stability. In vitro dissolution studies revealed a fourfold increase in drug dissolution for NIM-SD-SSNEDDS (84.43%) and NIM-SE-SSNEDDS (76.68%) compared to pure drug (28%). Ex vivo permeation studies indicated almost similar profiles for NIM-SD-SSNEDDS (22.61%) and NIM-SE-SSNEDDS (21.93%) compared to NIM-SNEDDS (25.02%).

Conclusion NIM-SD-SSNEDDS exhibited superior performance compared to NIM-SE-SSNEDDS, highlighting the efficacy of microparticles developed by the spray drying method (SD-CHEM) as adsorbents for solidification. These results suggest enhanced dissolution and permeation for nimodipine in both the solid SNEDDS.

Keywords Solid SNEDDS, Nimodipine, Flowability, Thermodynamic stability, In vitro dissolution, Ex vivo permeation

*Correspondence:
Pooja A. Chawla
pvchawla@gmail.com
Abdul Faruk
abdul_faruk@yahoo.com
Viney Chawla
drvineychawla@gmail.com
Full list of author information is available at the end of the article

Kumar *et al. Future Journal of Pharmaceutical Sciences*   (2024) 10:87

Page 2 of 17

Background

Self-nanoemulsifying drug delivery systems (SNEDDS) showcase a significant capacity for improving the oral bioavailability and biological efficacy of drugs characterized by poor water solubility [1, 2]. Lipid-based systems like SNEDDS have proven effective in addressing the problem of breakdown by enzymes in the gastrointestinal tract during the oral administration of biomolecules [3]. SNEDDS pose various challenges and obstacles, encompassing concerns related to both physical and chemical instability. The fluid nature of SNEDDS introduces several difficulties, such as constraints on dosage manufacturing, restricted choices for dosage forms, reduced drug loading capacity, and intricate issues in handling and storage [4, 5]. This leads the researchers to investigate various approaches to solidify SNEDDS, streamlining a swift and uncomplicated development of solidification of product with the desired properties [6].

There has been a growing emphasis on solid self-nanoemulsifying drug delivery systems (S-SNEDDS). These systems are formulated by integrating a liquid self-nanoemulsifying drug delivery system into a solid dosage form. This approach combines the benefits of SNEDDS with those of a solid dosage form, effectively addressing the limitations associated with liquid formulations [7]. S-SNEDDS offer a multitude of advantages, such as increased surface area leading to improved solubility and bioavailability, enhanced stability, robustness, easy handling, easy scale-up, enhanced drug loading capacity, better flow, minimized drug precipitation, and economical manufacturing [8]. SNEDDS suits BCS (Biopharmaceutical classification system) class II drugs (with low water solubility and high permeability), which have a dissolution-restricted absorption. This restricted absorption can result in a lack of success in therapeutic action because of insufficient drug concentration [9, 10].

Nimodipine (NIM), a BCS class II drug, is a calcium antagonist (dihydropyridine) with poor water solubility (2.30 μg/ml) and high lipophilicity and permeability (log $P = 3.41$) [11]. Because of the high lipophilicity, it can reach the brain and cerebrospinal fluid by crossing the blood–brain barrier [12]. It is highly used in the treatment of delayed ischaemic neurological disorder in patients with subarachnoid haemorrhage and cerebral vasospasm, stroke, senile dementia (due to irreversible loss of neurons) and hemicrania [13–16]. It has a moderate anti-hypertensive effect and is used in sudden sensorineural hearing loss [17].

Its mechanism of action is to block the entry of calcium through specific channels (voltage-dependent) and stop the contraction of vascular smooth muscles, leading to the dilation of the blood vessels [18].

NIM has two polymorphic forms and two enantiomers with different aqueous solubilities [19]. Because of the rapid first-pass metabolism and P-glycoprotein efflux, it has a lower oral bioavailability (around 13%) and requires high dosing (360 mg per day) [20]. Nimodipine was used as a model drug for developing the S-SNEDDS with chitosan-EDTA microparticles developed by spray drying and solvent evaporation techniques.

Materials and methods

Nimodipine was a gift sample from Strides Pharma Science limited (India). Cremophor® RH-40 (Polyoxyl 40 hydrogenated castor oil) was procured from Himedia (India). Lipoxol 300 (PEG 300) was procured from Sasol Chemicals (USA). Polyethylene glycol 400 (PEG 400) was obtained from TCI (India). Caprol® ET (hexaglycerol octasterate), Captex® 200 (propylene glycol dicaprylate), Captex® 300 (glyceryl tricaprylate/tricaprate) were gift samples from Abitech (USA). Labrafac™ PG (propylene glycol dicaprylocaprate) from Gattefossé (Canada) was received as a gift sample. Propylene glycol and Ethylene diamine tetra acetic acid disodium (EDTA disodium) were obtained from CDH (India). Chitosan with 90% deacetylation (DA) was acquired from Marine Hydrocolloids (India). Except for the ones we talked about, we used high-quality chemicals for the research. We used them just as they were, without any changes.

Drug solubility analysis in different excipients

As discussed, NIM is a high-dosing drug, so it becomes vital to obtain maximum drug loading in the SNEDDS. To create and chart the emulsification area, examining how much NIM could dissolve in various excipients was crucial. A surplus of the drug was placed in a sealed container, which was then subjected to a 40 °C water bath for 15 min. The mixture was stirred in an orbital shaker incubator (Remi, India) at 100 revolutions per minute for 72 h [21]. Subsequently, the mixture underwent centrifugation using a Remi RC-8 centrifuge from India at a speed of 4000–5000 rpm for 30 min. The resulting supernatant was filtered through Whatman filter paper with a pore size of 0.45 μm nylon. NIM was quantified at 237 nm using a UV spectrophotometer (UV–VIS spectrophotometer-2371 EI, India). The experimental procedure was repeated three times for accuracy [22].

The capacity for self-emulsification is an important factor when choosing excipients for SNEDDS, in addition to the drug's high solubility in both oil and surfactant. A 10% (w/v) aqueous solution of each surfactant (demonstrating significant high drug solubility) was created to assess this. Subsequently, 10 ml of this solution was titrated with each type of oil, and the volume of oil required to make the emulsion cloudy was recorded.

Kumar *et al. Future Journal of Pharmaceutical Sciences*   (2024) 10:87

Page 3 of 17

The combination of oil and surfactant that emulsified a maximum quantity (of oil) was chosen [23]. The selected surfactant (in a 1:1 ratio) with each co-surfactant (which had high drug solubility) was taken to form a mixture (Smix). Using this Smix, various formulations were created with the chosen oil, ranging from 10 to 90% in concentration. Each formulation, consisting of 500 mg, was individually mixed in 500 ml of triple distilled water, and the transparency or appearance of the mixture was then noticed [24].

Plotting of ternary phase diagram

We generated a ternary phase diagram to identify the suitable excipient range for creating nanoemulsion. Ternary mixtures, each totalling 1 g and including equal drug amounts, were prepared with three components. The selected surfactant and co-surfactant were combined in 1:1, 1:2, and 2:1 ratios, forming Smix mixtures. Subsequently, the oil and Smix were combined in nine different weight proportions, ranging from 1:9 to 9:1, in distinct glass vials. The aim was to determine the maximum limits for analysis to outline the phase accuracy boundaries in the diagram. Each formulation underwent titration with 500 ml of triple distilled water to observe nanoemulsion formation. The formation of a transparent/clear solution affirmed nanoemulsion creation. The proportions of oil and Smix were recorded and illustrated in the diagram. Chemix software was utilized for diagram plotting, with ingredients delineating the sides of this representation [25].

Development of self-nanoemulsifying drug delivery system

From the ternary phase diagram experiment, the appropriate proportions of oil and Smix were chosen to create a self-nanoemulsifying drug delivery system. The selected components were Cremophor RH 40 (as the oil), Lipoxol 300 (as the surfactant), and PEG 400 (as the co-surfactant). Subsequently, a liquid self-nanoemulsifying drug delivery system for Nimodipine (NIM-SNEDDS) was formulated. The measured amount of the drug was slowly introduced into the oil in a beaker and stirred at 2000 rpm on a magnetic stirrer until a homogeneous solution was achieved. Dropwise, adding a 1:1 Smix to this solution produced an isotropic mixture under continuous stirring for 30 min. The mixture was left to equilibrate for 48 h at room temperature, and observations were made for any phase separation [26].

Fabrication of SNEDDS to solid self-nanoemulsifying drug delivery system

Our earlier research optimized and created advanced adsorbent microparticles using chitosan-EDTA through spray drying (SD-CHEM) and a solvent evaporation method (SE-CHEM) [27]. These microparticles exhibited heightened abilities to absorb and release oil. Analysis of their surface free energy components revealed increased dispersive features and dynamic advancing contact angles, favourable characteristics for the adsorbent in converting liquid self-nanoemulsifying drug delivery systems (SNEDDS) into Solid SNEDDS (S-SNEDDS).

In the SE-CHEM process, a chitosan-EDTA disodium solution (60:40) underwent solvent evaporation in a Rota evaporator (Micro technologies, India) at a drying temperature of 70 °C for 45–60 min. Subsequently, the resulting dry film was carefully scraped, further dried in an oven for 40–50 min at 70 °C to eliminate residual moisture, and eventually converted into powder using a pestle and mortar. For SD-CHEM, a Chitosan-EDTA disodium solution (50:50) was processed in a Spray dryer (Spray-Mate JISL, India) with inlet temperature set at 110 °C, aspirator speed at 1000–2000 rpm, atomization pressure at 3 kg/cm^2, and feed pump operating at 15 rpm. In continuation to our research work, we fabricated the developed liquid SNEDDS of NIM with adsorption or solid carrier technique to create a solid self-nanoemulsifying drug delivery system (S-SNEDDS). The microparticles, created through SD-CHEM and SE-CHEM, served as adsorbents for the NIM-SNEDDS (nimodipine self-nanoemulsifying drug delivery system). Sequentially, NIM-SNEDDS was added to SD-CHEM and SE-CHEM individually and thoroughly mixed in a mortar and pestle. This process resulted in the formation of NIM-SD-SSNEDDS (nimodipine solid self-nanoemulsifying drug delivery system with spray-dried microparticles) and NIM-SE-SSNEDDS (nimodipine solid self-nanoemulsifying drug delivery system with solvent-evaporated microparticles) [27, 28]. The ratio of the adsorbate (NIM-SNEDDS) to adsorbent (SD-CHEM & SE-CHEM) was optimized to achieve non-sticky, free-flowing powders, namely NIM-SD-SSNEDDS and NIM-SE-SSNEDDS, respectively.

Different evaluations of the NIM-SNEDDS, NIM-SD-SSNEDDS, and NIM-SE-SSNEDDS

Drug loading efficiency (%)

To assess the drug loading efficiency (%), 100 mg of NIM-SNEDDS, NIM-SD-SSNEDDS, and NIM-SE-SSNEDDS was individually taken in 10 ml of methanol and vortexed in an orbital shaker (Remi, India) for 10 min. The NIM-SNEDDS mixture in methanol was directly analysed after appropriate dilution and examined at 237 nm using a UV spectrophotometer (UV–VIS spectrophotometer-2371 EI, India). The remaining two mixtures (NIM-SD-SSNEDDS and NIM-SE-SSNEDDS) were centrifuged (Remi Rc-8, India) at

4000 rpm for 10 min, and the supernatant obtained was filtered through Whatman filter paper (0.45 μm nylon). Following suitable dilution, these were analysed in a UV spectrophotometer, and the procedure was repeated in triplicate [28]. The drug loading efficiency (%) was calculated using the specified equation.

$$\text{Drug loading efficiency (\%)} = \frac{\text{Actual quantity of NIM present in the known amount of formulation}}{\text{Initial drug (NIM) load}} \times 100 \quad (1)$$

Flowability

For NIM-SD-SSNEDDS and NIM-SE-SSNEDDS, we determined the angle of repose using the fixed funnel method, along with apparent bulk density, tapped density, Carr's Index, and Hausner's ratio, employing standard methods to characterize their flow properties [29].

The angle of repose was determined by placing graph paper on a flat horizontal surface and clamping a funnel above it, maintaining a distance of approximately 7–8 cm between the paper and the funnel top. The powder samples (2 g) were measured and poured into the funnel until the top of the cone-shaped heap just reached the funnel's top. The height (h) and diameter of the cone-shaped heap of powder (D) were measured, and the angle of repose was calculated using the standard formula ($\tan \alpha = 2h/D$). A powder with an angle of repose less than 25° is considered to have excellent flow, while a powder with an angle of repose greater than 40° is considered to have poor flow.

The powder (2 g) was carefully weighed and levelled for bulk density determination without tapping into a graduated glass cylinder. The apparent volume before tapping read as an untapped volume using the USP method was considered for the standard formula (Bulk density = Weight/untapped volume), and values were calculated.

After 500 tapings, the volume of the powder-filled cylinder was measured. Tapping continued until the frequency difference between the two sets of tapping was less than 0.2 per cent. The final volume was noted, and the tapped density in g/ml was calculated using the standard formula (Tapped density = Weight/tapped volume).

These readings were then utilized to calculate Carr's index (CI) and Hausner's ratio (HR) using the formulas {CI = [(Tapped density − Bulk density/Tapped density) × 100] and HR = Tapped density/Bulk density}. Carr's index values above 25 indicate poor flowability, while values below 15 suggest good flowability. Hausner's ratios below 1.25 signify better flow properties than those above 1.25 [30].

Characterization (solid state)

X-ray diffraction analysis

Following the grinding of each sample (NIM, SD-CHEM, SE-CHEM, NIM-SD-SSNEDDS and NIM-SE-SSNEDDS), the resulting powder was placed and compacted in a sample holder. X-ray diffraction patterns of the samples were then measured using the X-ray diffractometer (XRD Aeris, Malvern Panalytical, UK). The continuous scanning of samples occurred within the range of 10°–50° at a rate of 2° per minute, with 0.02° 2θ increments. The scanning process commenced at 5° and concluded at 50° (2θ), with the scans conducted at 25 °C and the generator configured at 45 kV [28].

Scanning electron microscopy

The surface characteristics of NIM, SD-CHEM, SE-CHEM, NIM-SD-SSNEDDS, and NIM-SE-SSNEDDS were examined using the scanning electron microscope (SEM) (ZEISS Sigma 360, Germany) at 20 kV. The samples were affixed to the SEM stub and coated with a thin layer of gold. Multiple images were captured at various magnifications [30].

FTIR spectroscopy

Different components of the formulations, as well as their physical mixtures, were examined for possible incompatibilities. To create a fine mixture, the prepared samples were dried under vacuum, mixed, and triturated with KBr at a 1:100 ratio. Pellets were formed by pressing this fine mixture in a KBr press. Subsequently, these pellets were placed in a sample cell, and FTIR-ATR analysis was conducted (FTIR Perkin Elmer Spectrum Two, USA) in the 500–4000 cm^{-1} spectral range at room temperature [31].

DSC analysis

Hermetically sealed aluminium pans containing samples (15 mg each) of NIM, NIM-SNEDDS, NIM-SD-SSNEDDS, and NIM-SE-SSNEDDS were utilized. These pans were positioned on the sample pan holder, while empty pans were placed on the reference pan holders in a differential scanning calorimeter (DSC-25 TA, USA). Thermograms for each sample were then recorded within a temperature range of 40–400 °C, employing a heating rate of 10 °C per minute in a nitrogen atmosphere.

Kumar *et al. Future Journal of Pharmaceutical Sciences*   (2024) 10:87

Page 5 of 17

Reconstituted nanoemulsion and NIM-SNEDDS evaluations

To assess reconstitution ability, 100 mg of NIM-SD-SSNEDDS and NIM-SE-SSNEDDS was dispersed separately in 100 ml of triple distilled water for 1 h. Subsequently, the dispersions were vortexed in an orbital shaker (Remi, India) for 10 min. The resulting suspension underwent centrifugation (Remi RC-8, India) at 4000 rpm for 10 min to eliminate undissolved particles. The obtained supernatant was reconstituted nanoemulsion and utilized for subsequent investigations. Additionally, a 1:100 w/v dilution of freshly prepared NIM-SNEDDS with triple distilled water was created, dispersed, and used for further analysis.

Droplet size, size distribution, and zeta potential determination

The size of the droplets, polydispersibility index, and zeta potential of the reconstituted nanoemulsions and NIM-SNEDDS were examined using the Zetasizer Nano ZS (at a wavelength of 633 nm) with a scattering angle of 90° at 25 °C. The analysis was conducted in triplicate using equipment from Malvern Panalytical, UK [32, 33].

Self-emulsification time

The NIM-SD-SSNEDDS and NIM-SE-SSNEDDS supernatants and NIM-SNEDDS (1 ml each) were dispersed in 500 ml of triple distilled water and stirred at approximately 100 rpm using a magnetic stirrer. Observations were made to determine the formation of emulsion and the time needed for dispersibility [34].

Per cent transmittance test

When formulating self-nanoemulsifying drug delivery systems for oral administration, drug precipitation is possible upon dilution in the gastrointestinal tract. To assess this, the supernatants of NIM-SNEDDS, NIM-SD-SSNEDDS, and NIM-SE-SSNEDDS were tested for per cent transmittance at 237 nm, with water as the blank, using a UV spectrophotometer (UV–VIS spectrophotometer-2371 EI, India). The test was conducted in triplicate for accuracy [35, 36].

Estimation of cloud point

The supernatants (NIM-SD-SSNEDDS and NIM-SE-SSNEDDS) and NIM-SNEDDS were subjected to a water bath with a gradual temperature increase. The temperature at which immediate turbidity was observed in the samples was recorded [37].

Field emission scanning electron microscopy

The supernatant (50 μl) of both NIM-SD-SSNEDDS and NIM-SE-SSNEDDS was drop-casted onto glass slides that had been cleaned beforehand. The dried samples were then gold-coated using a sputter-coater for 10–15 s under high vacuum conditions. High-resolution images were captured at 15 kV using an accelerating voltage in field emission scanning electron microscopy (FE-SEM) (Quanta 250, Bruker) [38].

Dissolution profile (in vitro)

For assessing the dissolution release of NIM, the pure NIM, NIM-SNEDDS, NIM-SD-SNEDDS, and NIM-SE-SNEDDS, equivalent to 10 mg, were individually filled into hard gelatin capsules. The release study used the USP dissolution apparatus II-paddle at 37 ± 0.5 °C (Electrolab India, India) in pH 4.5 acetate buffer as the dissolution medium, stirring at 50 rpm. At various time intervals, 2 ml of sample aliquot was withdrawn (instantly filtered), and fresh medium was added to maintain sink conditions. After appropriate dilution with pH 4.5 acetate buffer, samples were analysed at 237 nm using a UV spectrophotometer [39]. The experiments were repeated three times to ensure consistent and accurate results.

Ex vivo permeability profile

The ex vivo permeation method was applied, as described by Singh et al. [40]. In summary, the ex vivo permeation method involved utilizing the biological membrane from the porcine small intestine acquired from a local slaughterhouse in Srinagar Garhwal, Uttarakhand, India. The intestine, obtained within one hour of slaughter, was preserved in Kreb's ringer phosphate solution at 4 °C with aeration. A 10–12-cm section of the intestine was dissected, washed with saline, and placed on saline-soaked filter paper. After making a lengthwise cut to flatten it, the serosal membrane faced upward, and the muscle layer was removed using a scalpel. For the permeation study, the intestine member was mounted in a modified Franz diffusion cell with the mucosal layer facing the donor compartment side. A pH 4.5 acetate buffer in the receptor compartment served as the receptor medium, maintained at 37 ± 0.5 °C and stirred at 50 rpm. The donor compartment received pure NIM/NIM-SNEDDS/NIM-SD-SSNEDDS/NIM-SE-SSNEDDS (equivalent to 5 mg of NIM) on the mucosal side of the membrane. At various time intervals, a 1 ml sample was withdrawn and replaced with a fresh 1 ml pH 4.5 acetate buffer in the receptor compartment. The samples were analysed at 237 nm using a UV spectrophotometer after appropriate dilution to determine the amount of NIM diffused through the membrane. The experiments were repeated three times to ensure a consistent and accurate average value.
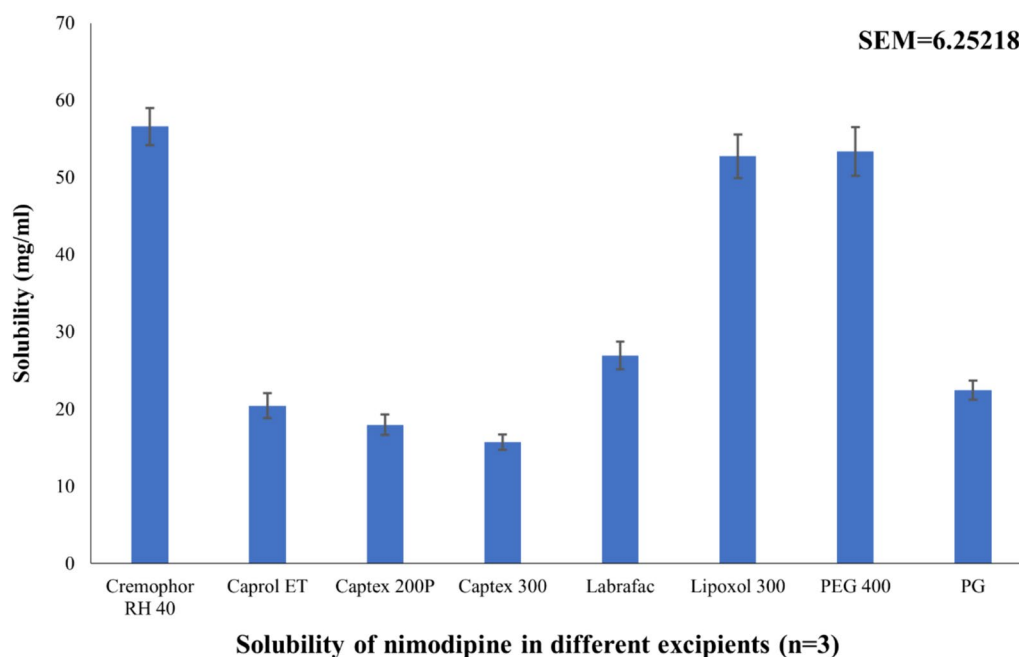
Fig. 1 Solubility of nimodipine in different excipients (mg/ml)

Stability study

The HDPE bottles (60 ml) containing 40 capsules of each NIM-SD-SSNEDSS and NIM-SE-SSNEDDS (each capsule equivalent to 20 mg of nimodipine) were subjected to accelerated conditions (40 ± 2 °C/$75 \pm 5\%$ RH) in a stability (humidity) chamber (Newtronic, India) for six months post-sealing. Throughout this period, samples were periodically withdrawn and examined for physical appearance, percentage cumulative drug release (% CDR), and disintegration time [41].

Results

Drug solubility analysis in different excipients

Formulations often encounter the challenge of precipitation before undergoing in situ solubilization. Hence, to verify the stability of the formulation, understanding the drug's solubility in the chosen excipients becomes crucial. High drug solubility in various formulation excipients is essential for achieving optimal drug loading and bioavailability [42]. For the development of an effective SNEDDS for NIM, it is essential that the drug readily mixes with the selected excipients, minimizing its incorporation into the mixture [43]. Figure 1 illustrates the solubility of NIM in different excipients.

To achieve effective self-emulsification, it is essential to have the optimal combination of excipients. Analysis of the self-emulsification potential demonstrated that Lipoxol 300, combined with the highest quantity of
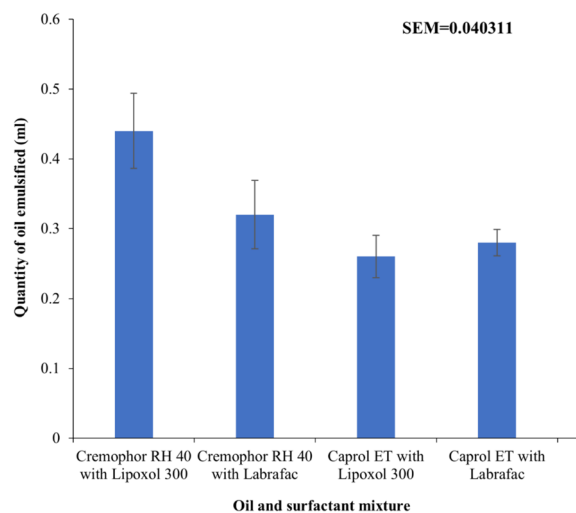
Fig. 2 Self-emulsification of oils with surfactants ($n=3$)

Cremophor RH 40, resulted in successful emulsification, as illustrated in Fig. 2.

Upon perceiving this finding, Cremophor RH 40 and Lipoxol 300 were chosen as the oil and surfactant, respectively. Polyethylene glycol 400 (PEG 400) was selected as the co-surfactant based on the broader range of nanoemulsion regions observed compared to propylene glycol (PG), as depicted in Table 1.

Increased surfactant levels can boost the self-emulsification process. Including a co-surfactant, such as

Kumar *et al. Future Journal of Pharmaceutical Sciences*   (2024) 10:87

Page 7 of 17

Table 1 Nanoemulsion region formation (Smix with different co-surfactants)

Composition		Nanoemulsion region	
Oil (%)	S_{mix} (%)	S_{mix} of Lipoxol 300: PEG 400 (1:1)	S_{mix} of Lipoxol 300: PG (1:1)
10	90	Yes	Yes
20	80	Yes	Yes
30	70	Yes	Yes
40	60	Yes	Yes
50	50	Yes	No
60	40	No	No
70	30	No	No
80	20	No	No
90	10	No	No

PEG 400 polyethylene glycol 400, *PG* propylene glycol

PEG 400, does not compromise the surfactant's ability to decrease interfacial tension around the oily component. Utilizing a co-surfactant allows for a reduction in the overall amount of surfactant in the formulation [44]. In this specific formulation, PEG 400 serves as the co-surfactant.

Plotting of ternary phase diagram

In order to select the right proportion of excipients for self-nanoemulsifying drug delivery systems (SNEDDS) and observe self-emulsification in the nano-range, a ternary phase diagram was constructed with the inclusion of NIM. This diagram aids in comprehending the phase behaviour of nanoemulsions [45].

The water-titration method was employed to create a diagram, incorporating an oily vehicle ranging from 10 to 90% and varying Smix ratios (1:1, 1:2, and 2:1). Transparent regions, indicating nanoemulsion areas were identified, and ternary diagrams were constructed using this information, specifically for three Smix ratios (1:1, 1:2, and 2:1). The shaded portions in Fig. 3a–c represent the transparent nanoemulsion regions with low viscosity. In diagrams, each peak denotes 100% of the corresponding excipient.

According to Fig. 3a (for oil and Smix 1:2), when the oil content is less and PEG 400 is more, the shaded nanoemulsion region is observed, and when the oil content is increased and PEG 400 is reduced, the biphasic system can be seen. In the case of Smix 2:1 with oil, the increase in Lipoxol 300 gives a greater nanoemulsion area (in Fig. 3b). As per Fig. 3c, (oil and Smix 1:1) the 30–50% of Cremophor RH 40, and less percentage of Smix is resulting in a nanoemulsion region. When PEG 400 increases, the nanoemulsion region is reduced because of the
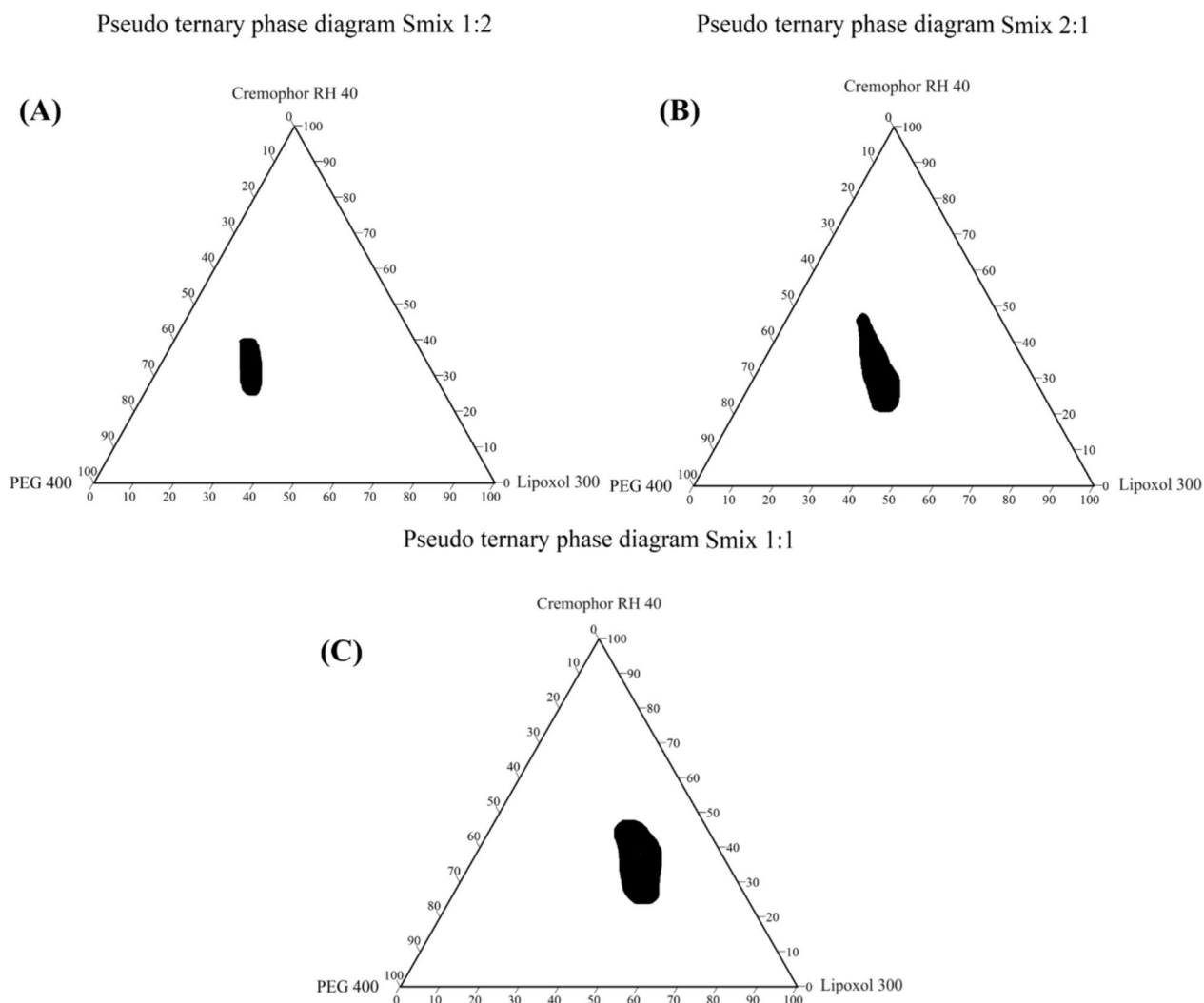
limited capability of PEG 400 to the interfacial tension. At the same time, Lipoxol 300 has a greater effect of reducing the interfacial tension by making a layer around the oil droplets. The Smix ratio of 1:1, serving as a surfactant/co-surfactant mixture, was identified as suitable.

Development of self-nanoemulsifying drug delivery system and fabrication of SNEDDS to solid self-nanoemulsifying drug delivery system

Based on the findings from the two studies of the ternary phase diagram (Fig. 3c) and nanoemulsion region formation (Table 1), it was clear that a 40:60 ratio of oil (Cremophor RH 40) to Smix (Lipoxol 300: PEG 400 = 1:1; serving as a surfactant/co-surfactant mixture), was producing nanoemulsion. This 40:60 ratio had a significant amount of oil (part), which remains essential for maximum drug solubilization and high drug loading into the formulation. Hence, this was chosen for the development of the SNEDDS development. Following the outlined procedure, the liquid NIM-SNEDDS was created and stored in an airtight container. The ultimate composition of NIM-SNEDDS consisted of 100 mg of NIM, 400 mg of Cremophor RH 40, 300 mg of Lipoxol 300, and 300 mg of PEG 400. The microparticles created through spray drying (SD-CHEM) and the chitosan EDTA microparticles using the solvent evaporation method (SE-CHEM) showcased their capabilities with high oil adsorption and desorption capacities. These microparticles also demonstrated favourable enhancements in surface free energy components and dynamic advancing contact angles. The solid self-nanoemulsifying drug delivery systems (S-SNEDDS) were independently formulated for both SD-CHEM and SE-CHEM through an adsorption or solid carrier technique. Among the two ratios of adsorbate (NIM-SNEDDS) to adsorbent (SD-CHEM), namely 1:1.5 and 1:2.5, the 1:2.5 ratio was identified as yielding a non-sticky, free-flowing powder for NIM-SD-SSNEDDS. For NIM-SE-SSNEDDS, considering two ratios of adsorbate (NIM-SNEDDS) to adsorbent (SE-CHEM), namely 1:2 and 1:2.5, the 1:2.5 ratio was determined to result in a non-sticky, free-flowing powder. This adsorption technique is particularly advantageous for thermolabile drugs as it avoids subjecting the system to heat treatment. The resultant NIM-SD-SSNEDDS, NIM-SE-SSNEDDS, and NIM-SNEDDS (liquid) were subsequently assessed.

Different evaluations of the NIM-SNEDDS, NIM-SD-SSNEDDS, and NIM-SE-SSNEDDS

Drug loading efficiency (%)

As indicated in Table 2, the drug loading efficiency for NIM-SD-SSNEDDS and NIM-SE-SSNEDDS was found to be $79.67 \pm 2.97\%$ and $77.76 \pm 4.29\%$, respectively. As anticipated, the drug loading efficiency (%) for

Pseudo ternary phase diagram Smix 1:2

Pseudo ternary phase diagram Smix 2:1

Pseudo ternary phase diagram Smix 1:1

Fig. 3 Pseudo ternary phase diagrams **A** with Smix 1:2, **B** with Smix 2:1, and **C** with Smix 1:1

NIM-SNEDDS was $82.75 \pm 3.56\%$. Notably, a certain loss in drug loading occurred during the solidification process from NIM-SNEDDS to NIM-SD-SSNEDDS and NIM-SE-SSNEDDS using the adsorption technique.

Flowability
For NIM-SD-SSNEDDS and NIM-SE-SSNEDDS, the resulting flow properties were calculated and are presented in Table 2. The bulk density of NIM-SD-SSNEDDS and NIM-SE-SSNEDDS was 0.893 ± 0.209 g/cm^3 and 0.758 ± 0.116 g/cm^3, indicating the presence of gaps between powder particles, which is crucial in the industry (for efficient capsule filling). The tapped density for NIM-SD-SSNEDDS and NIM-SE-SSNEDDS was 0.928 ± 0.194 g/cm^3 and 0.752 ± 0.116 g/cm^3. The minimal difference between these densities (bulk and tapped), along

with Carr's index (NIM-SD-SSNEDDS = 5.119 ± 0.083 and NIM-SE-SSNEDDS = 13.588 ± 0.236), Hausner's ratio (NIM-SD-SSNEDDS = 1.051 ± 0.074 and NIM-SE-SSNEDDS = 1.135 ± 0.071), and angle of repose (NIM-SD-SSNEDDS = 10.752 ± 2.145 and NIM-SE-SSNEDDS = 9.734 ± 1.921), signifies excellent flow properties for the formulations.

Characterization (solid state)
X-ray diffraction analysis
Detecting changes in polymorphism, dissolution rate (solubility), and stability depends on the critical quality attribute of particle crystallinity, as determined by XRD analysis. Figure 4 illustrates the X-ray diffraction (XRD) analysis of NIM, SD-CHEM, SE-CHEM, NIM-SD-SSNEDDS, and NIM-SE-SSNEDDS. NIM exhibited diffraction peaks at 2θ values of 12.53°, 13.06°, 17.54°,

Table 2 Flow properties, physical characterization, dissolution, and permeation profiles of the formulations

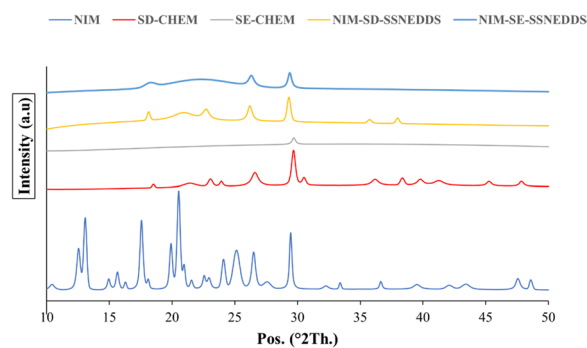|	NIM-SNEDDS	NIM-SD-SSNEDDS	NIM-SE-SSNEDDS
Flow properties			
Bulk density (g/cm^3)	–	0.893 ± 0.209	0.752 ± 0.116
Tapped density (g/cm^3)	–	0.928 ± 0.194	0.861 ± 0.251
Carr's index (%)	–	5.119 ± 0.083	13.588 ± 0.236
Hausner's ratio	–	1.051 ± 0.074	1.135 ± 0.071
Angle of repose(θ)	–	10.752 ± 2.145	9.734 ± 1.921
Flowability	–	Good	Good
Physical characterization			
Droplet size (nm)	245.5 ± 3.745	247.1 ± 3.282	399.6 ± 3.851
PDI	0.715 ± 0.008	0.620 ± 0.003	0.821 ± 0.005
Zeta potential (mV)	1.961 ± 0.426	1.353 ± 0.073	1.351 ± 0.853
Emulsification time (sec)	24–36	38–41	40–48
% transmittance	98.192 ± 0.141	94.645 ± 0.628	92.962 ± 0.932
Cloud temp. (℃)	69	54	49
Dissolution profiles			
Drug loading efficiency (%)	82.757 ± 3.561	79.675 ± 2.973	77.763 ± 4.292
Dissolution efficiency (%)	88.84	84.43	76.68
Permeation profile			
Ex-vivo permeation efficiency (%)	25.026	22.609	21.932
Flux	3.692	3.186	3.305
Permeability constant	0.738	0.637	0.661

Values are presented as mean ± standard deviation (S.D.), ($n = 3$)

19.89°, 20.51°, 25.11°, and 29.43°. These peaks align with the distinctive crystalline pattern of NIM [19]. The SD-CHEM samples exhibited diffraction peaks at 2θ values of 18.51°, 21.41°, 26.61°, and 29.67°. In the SE-CHEM samples, almost indistinct diffraction peaks at 2θ values of 21.2° and 23° were observed, along with significantly broadened peaks at 26.5° and 29.8°. For NIM-SD-SSNEDDS, diffraction peaks were observed at 2θ values of 18.11°, 20.9°, 22.69°, 26.18°, and 29.28°. NIM-SE-SSNEDDS displayed diffraction peaks at 2θ values of 18.24°, 22.26°, 26.30°, and 29.36°. The absence of distinctive crystalline peaks of NIM in solid SNEDDS suggests the amorphization of the drug in the formulation. This amorphization, coupled with nanometric sizes and the absence of crystallinity, contributes to the anticipated improved dissolution behaviour in self-nanoemulsifying formulations. Importantly, the investigation indicates no signs of NIM precipitation when incorporated into S-SNEDDS.

Scanning electron microscopy

To comprehend the structure and surface characteristics of the solid formulations, scanning electron microscope (SEM) images of NIM, SD-CHEM, SE-CHEM, NIM-SD-SSNEDDS, and NIM-SE-SSNEDDS were captured (as


Fig. 4 XRD analysis of NIM, SD-CHEM, SE-CHEM, NIM-SD-SSNEDDS, and NIM-SE-SSNEDDS

depicted in Fig. 5). In Fig. 5 (a,b), the pure NIM sample is illustrated, and Fig. 5c displays SD-CHEM, exhibiting a spherical shape with uneven surfaces and substantial void spaces, facilitating effective oil adsorption and desorption. Figure 5d showcases SE-CHEM, presenting a flaky appearance with an irregular surface, providing an increased surface area for the adsorption of liquid SNEDDS. Figure 5e depicts NIM-SD-SSNEDDS with a size range of 10–15 µm. The adsorption process with NIM-SNEDDS is evident in these images, as seen by the smoothing of uneven surfaces and void spaces present
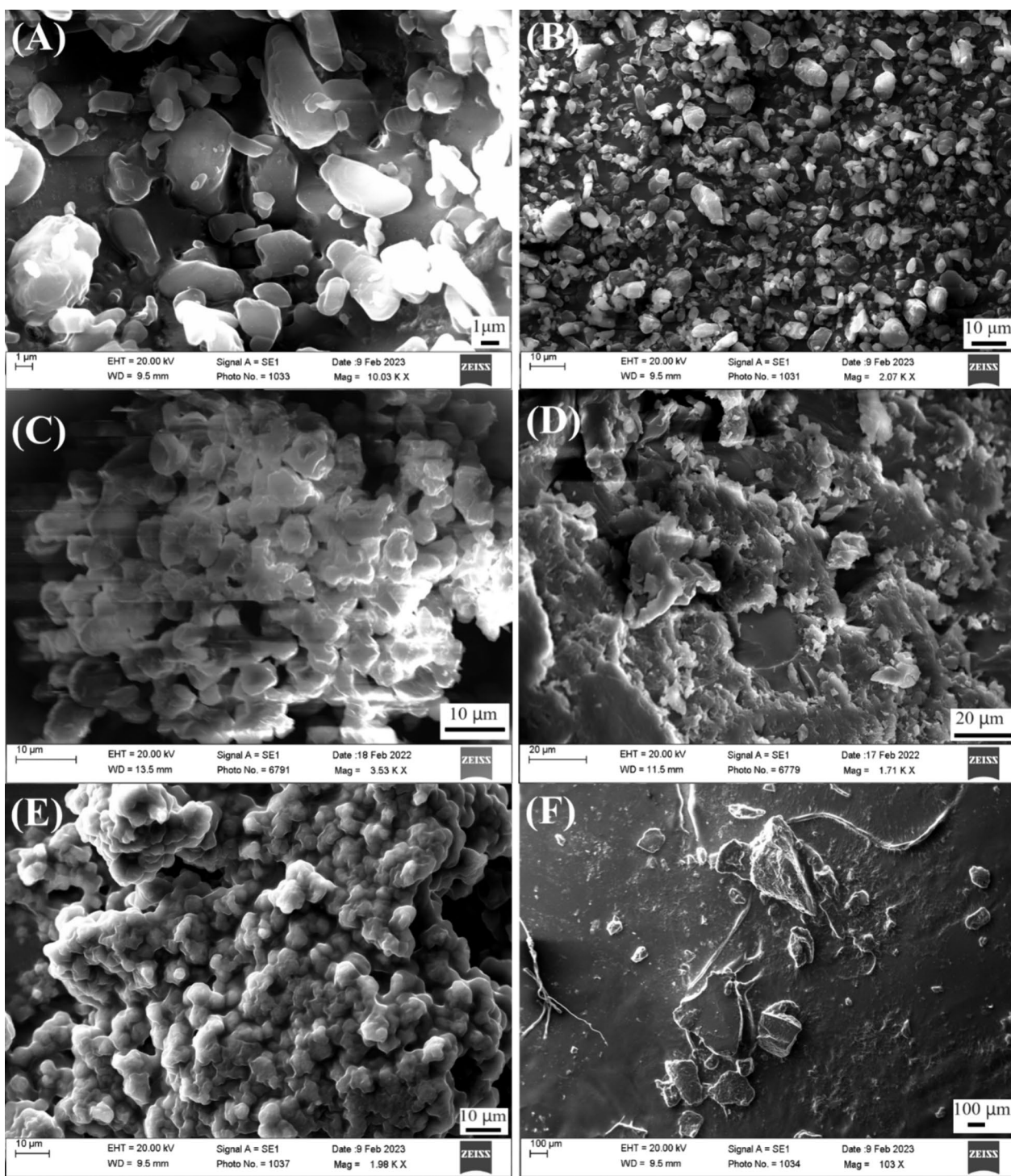
Fig. 5 Surface morphology of **A** and **B** NIM, **C** SD-CHEM, **D** SE-CHEM, **E** NIM-SD-SSNEDDS, and **F** NIM-SE-SSNEDDS
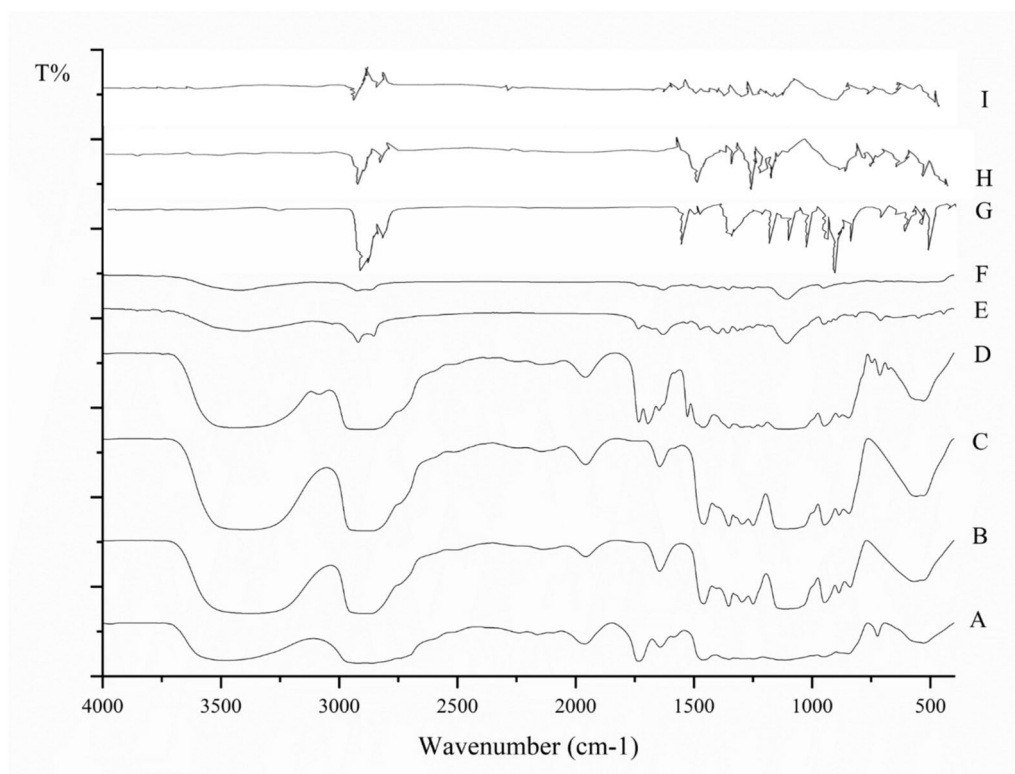
Fig. 6 FTIR spectra of **A** Cremophor RH 40, **B** Lipoxol 300, **C** PEG 400, **D** NIM-SNEDDS, **E** NIM-SD-SSNEDDS, **F** NIM-SE-SSNEDDS, **G** NIM, **H** SD-CHEM, and **I** SE-CHEM

in SD-CHEM. Likewise, in Fig. 5f, NIM-SE-SSNEDDS exhibits smooth, flaky structures compared to SE-CHEM, with a 20–25 µm size range.

FTIR spectroscopy

Figure 6 shows all the FTIR spectra. The absorption bands of 3390.4 cm^{-1}, 3371.4 cm^{-1} and 3391 cm^{-1} confirm the O–H stretching, and the absorption bands 2922.1 cm^{-1}, 2875.3 cm^{-1}, and 2873.5 cm^{-1} correspond to the C–H bonds, the absorption peaks, 1249.5 cm^{-1}, 1249.6 cm^{-1} and 1249.4 cm^{-1} confirms the C–O–C stretching (ether) in Cremophor RH 40, Lipoxol 300 and PEG 400, respectively [46–48]. The absorption peak at 1782.5 cm^{-1} confirms the carbonyl group (of ester) in Cremophor RH 40. The absorption bands near 1457 cm^{-1} confirm CH$_2$ with bending vibrations in Lipoxol 300 and PEG 400, respectively. SE-CHEM and SD-CHEM displayed absorption bands within the range of 1676–1657 cm^{-1} and 1693–1667 cm^{-1}, respectively, indicating the presence of the amide linkage. Additionally, they exhibited absorption bands between 2378 and 2373 cm^{-1}, suggesting the presence of free acetate moieties. This implies that not all acetate moieties are engaged in the amide linkage. The FTIR spectra of NIM showed all the fingerprint bands

of it [49]. The absorption band at 3295.2 cm^{-1} confirms the presence of primary and secondary amines, indicated by N–H stretching vibrations. The absorption band within the 2967.4–2879.5 cm^{-1} range corresponds to alkyl groups, specifically C–H stretching vibrations. The absorption band at 1693.4 cm^{-1} confirms the presence of the ester group, as indicated by C=O stretching vibration. Furthermore, 1645 cm^{-1} and 1620 cm^{-1} absorption bands confirm C=C stretching and C=C aromatic functionalities. Additionally, absorption bands at 1521.4 cm^{-1}, 1381.9 cm^{-1}, and 1133.2 cm^{-1} are attributed to –NO$_2$, –C–CH$_3$, and –C–O– ester, respectively.

In the spectra of NIM-SNEDDS, NIM-SD-SSNEDDS, and NIM-SE-SSNEDDS, no notable changes were observed concerning the characteristic peaks of NIM. In the NIM-SNEDDS spectra, absorptions were detected at 3440.5 cm^{-1}, 3085.6 cm^{-1}, 2871.2 cm^{-1}, 1647.1 cm^{-1}, 1460 cm^{-1}, and 1108.9 cm^{-1}. The NIM-SD-SSNEDDS spectra exhibited absorptions at 3392.6 cm^{-1}, 2919 cm^{-1}, 2853.5 cm^{-1}, 1629.3 cm^{-1}, 1472 cm^{-1}, and 1106.7 cm^{-1}. Similarly, the NIM-SE-SSNEDDS spectra displayed absorptions at 3424.1 cm^{-1}, 2923.3 cm^{-1}, 1629.3 cm^{-1}, 1459.6 cm^{-1}, and 1107 cm^{-1}. Some peaks exhibited broadening and negligible shifts, potentially attributed
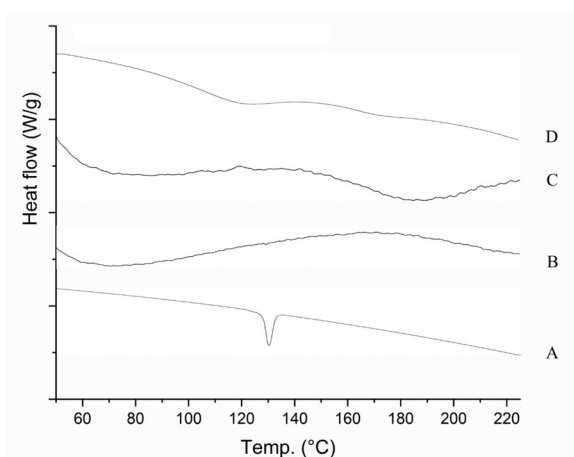
Fig. 7 DSC curves of **A** NIM, **B** NIM-SNEDDS, **C** NIM-SD-SSNEDDS, and **D** NIM-SE-SSNEDDS

to hydrogen bonding between the drug and surfactants [19]. The occurrence of hydrogen bonding could lead to shifts in wavelengths, reducing intensities, or even causing peaks to disappear [50].

DSC analysis
DSC analysis was employed to detect potential polymorphic changes induced by the interaction between the drug and excipients. The thermograms of NIM, NIM-SNEDDS, NIM-SD-SSNEDDS, and NIM-SE-SSNEDDS were obtained and are presented in Fig. 7. The characteristic endothermic peak of NIM, signifying its crystallinity, was observed at 128 °C [51]. In NIM-SNEDDS and NIM-SD-SSNEDDS, this endothermic peak disappeared, while in NIM-SE-SSNEDDS, a broad peak near 128 °C was observed. The disappearance of the characteristic endothermic peak indicates that the NIM is in amorphous form in formulations.

Reconstituted nanoemulsion and NIM-SNEDDS evaluations
Droplet size, size distribution, and zeta potential determination
Determining droplet size is crucial in assessing the self-nanoemulsification characteristics of the system, as it influences drug release and absorption. Smaller droplet sizes in the nanometric range provide a larger interfacial surface area, facilitating better drug absorption. In Table 2, the droplet sizes (and polydispersibility index-PDI) of NIM-SNEDDS, NIM-SD-SSNEDDS, and NIM-SE-SSNEDDS are 245.5 nm (PDI–0.715), 247.1 nm (PDI–0.620), and 399.6 nm (PDI–0.821). The results show that the droplet size of NIM-SD-SSNEDDS is comparable to NIM-SNEDDS, while NIM-SE-SSNEDDS exhibits a significant difference. PDI values for all formulations are

closely aligned. Thus, SD-CHEM and SE-CHEM surfaces exhibit small droplet sizes and similar PDI. SD-CHEM (NIM-SD-SSNEDDS), as an adsorbent, outperforms SE-CHEM in producing small droplets and PDI. The zeta potential results for NIM-SNEDDS, NIM-SD-SSNEDDS, and NIM-SE-SSNEDDS are 1.961 mV, 1.353 mV, and 1.351 mV, respectively.

Self-emulsification time
The emulsification times for NIM-SNEDDS, NIM-SD-SSNEDDS, and NIM-SE-SSNEDDS were recorded as 24–36, 38–41, and 40–48 s, respectively, as outlined in Table 2. This indicates that all systems possess the capability to disperse swiftly in aqueous conditions with agitation.

Per cent transmittance test
The outcomes of per cent transmittance for NIM-SNEDDS, NIM-SD-SSNEDDS, and NIM-SE-SSNEDDS, as depicted in Table 2, exceeded 90%, substantiating the effectiveness of self-emulsification. This transparency further validates the stability of the reconstituted nanoemulsion and eliminates the risk of drug precipitation [52].

Estimation of cloud point
The cloud point temperature signifies the temperature at which the clear appearance of the SNEDDS transforms into a cloudy or turbid state, indicating a change in phase behaviour. This temperature should ideally be higher than the anticipated usage temperature, typically 37 °C. In the case of NIM-SNEDDS, NIM-SD-SSNEDSS, and NIM-SE-SSNEDDS, all recorded cloud point temperatures were above 37 °C, affirming their thermodynamic stability [53].

Field emission scanning electron microscopy
The FE-SEM images in Fig. 8a–c illustrate the reconstituted NIM-SD-SSNEDDS, while Fig. 8d–f displays NIM-SE-SSNEDDS, both captured at various magnifications. The images clearly depict that the reconstituted globules from both solid SNEDDS forms were spherical. Additionally, these images corroborate with the sizes analysed through Zetasizer, as indicated in Table 2. The globules formed exhibited fine sizes, and there was no coalescence evidence, implying the reconstituted nanoemulsions' stability.
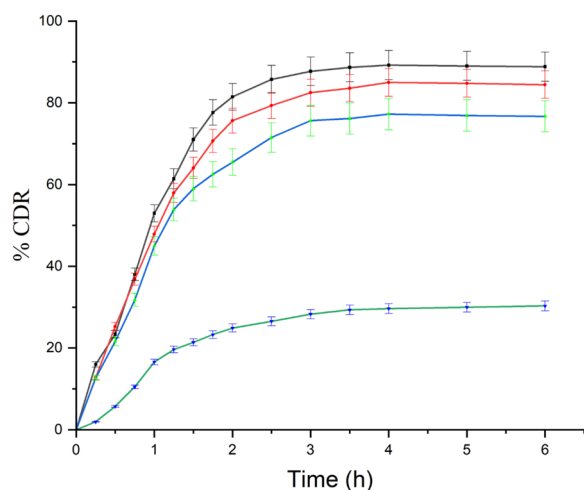
Dissolution profile (in vitro)
The in vitro dissolution test investigated the release of pure NIM, NIM-SNEDDS, NIM-SD-SSNEDDS, and NIM-SE-SSNEDDS, with the per cent cumulative drug release (% CDR) graph displayed in Fig. 9. In six hours, the % CDR for pure NIM, NIM-SNEDDS,
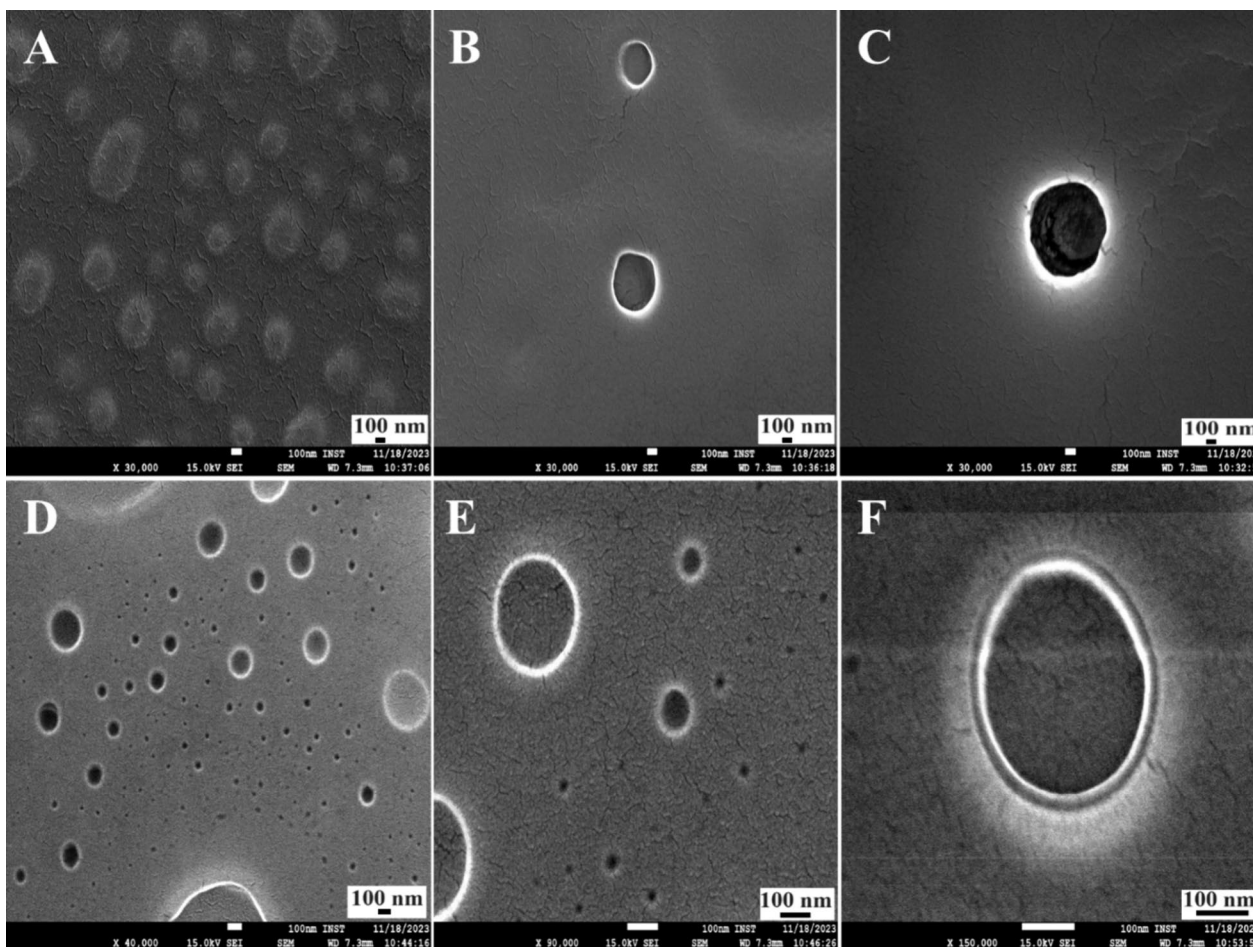
Fig. 8 FE-SEM images (at different magnifications) **A**, **B,** and **C** reconstituted nanoemulsion NIM-SD-SSNEDDS, **C** and **D** reconstituted nanoemulsion NIM-SE-SSNEDDS
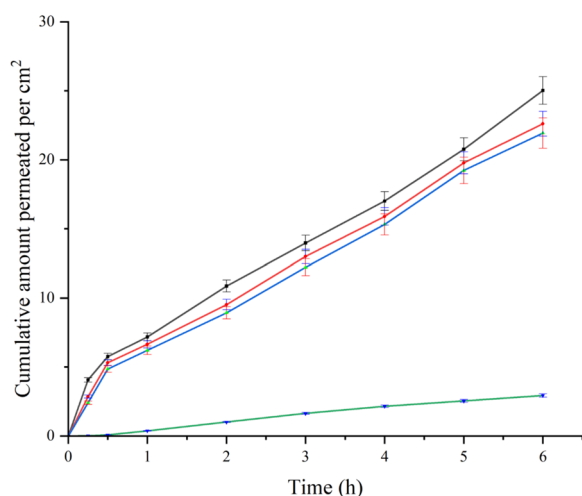

Fig. 9 Dissolution profile (% cumulative drug release) of **A** NIM **B** NIM-SE-SSNEDDS, **C** NIM-SD-SSNEDDS, and **D** NIM-SNEDDS

NIM-SD-SSNEDDS, and NIM-SE-SSNEDDS was 28%, 88.84%, 84.43%, and 76.68%, respectively. Notably, there was a significant increase in drug dissolution for NIM in both NIM-SD-SNEDDS and NIM-SE-SSNEDDS compared to pure NIM. This study has revealed the improvement of dissolution of the drug after formulating into the SNEDDS and S-SNEDDS, this must be due to the loading of the drug into the micelles of the SNEDDS [54].

Ex vivo permeability profile

This investigation assessed drug permeability through a biological membrane as a diffusion barrier. A comparative analysis was conducted for pure NIM, NIM-SNEDDS, reconstituted NIM-SD-SSNEDDS, and NIM-SE-SSNEDDS. Figure 10 presents the cumulative amount permeated per cm^2, while Fig. 11 illustrates the flux and permeability constant. Flux, represented as the drug permeated per unit area per unit time (µg/

Kumar *et al. Future Journal of Pharmaceutical Sciences* (2024) 10:87

Page 14 of 17

Fig. 10 Ex vivo permeation profile of **A** NIM **B** NIM-SE-SSNEDDS, **C** NIM-SD-SSNEDDS, and **D** NIM-SNEDDS
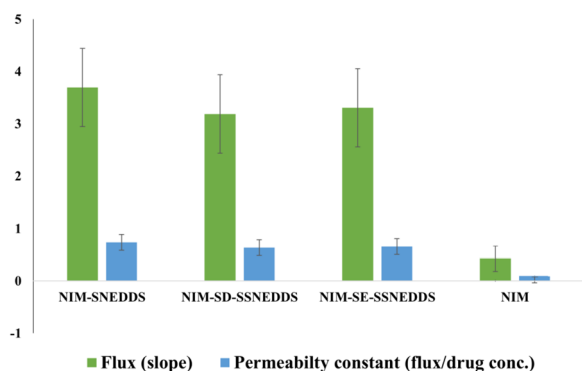
Fig. 11 Ex vivo permeation parameters of NIM, NIM-SE-SSNEDDS, NIM-SD-SSNEDDS, and NIM-SNEDDS. Flux refers to the quantity of drug that permeates a diffusion barrier per unit area and time, expressed as micrograms per minute per square centimetre (μg/min/cm^2) $\times 10^{-2}$ (the slope of the permeability curve). The permeability constant is calculated as the ratio of flux to drug concentration

min/cm^2) $\times 10^{-2}$ (slope of the permeability curve), and permeability constant, defining the ease of drug diffusion from the permeable membrane (flux/drug conc.), were evaluated. The results indicated that the cumulative drug permeability (%) for NIM, NIM-SNEDDS, NIM-SD-SSNEDDS, and NIM-SE-SSNEDDS was 2.93, 25.02, 22.6, and 21.9, respectively. In Fig. 11, higher values of both flux and permeability constant of NIM-SNEDDS, NIM-SD-SSNEDDS, and NIM-SE-SSNEDDS as compared to NIM, indicated the enhancement in permeation across the biological membrane and facilitation of the drug across the membrane by SNEDDS and S-SNEDDS, respectively.

Stability study

The summarized results of the stability study are presented in Table 3. Analysis of the data reveals that both formulations, NIM-SD-SSNEDDS and NIM-SE-SSNEDDS, remained stable throughout the six-month accelerated stability testing at 40 ± 2 °C/75 $\pm$ 5% RH. Therefore, it can be concluded that both NIM-SD-SSNEDDS and NIM-SE-SSNEDDS successfully passed the stability assessment.

Discussion

Because of the number of advantages of solid SNEDDS over SNEDDS, this study aimed to formulate solid self-nanoemulsifying drug delivery systems (S-SNEDDS) for nimodipine (NIM). NIM used as a model drug remains a suitable candidate for SNEDDS due to low hydrophilicity and high lipophilicity. Cremophor RH 40, Lipoxol 300, and PEG 400 were chosen after checking how well they dissolve and form emulsions. A ternary phase diagram determined the optimal oil to Smix (surfactant/co-surfactant) ratio (40:60). The liquid NIM-SNEDDS was used as the material to adsorb on microparticles synthesized from chitosan EDTA by spray drying (SD-CHEM) and solvent evaporation (SE-CHEM) as the absorbents to make solid SNEDDS. Both solid forms had good drug loading (NIM-SD-SSNEDDS $= 79.67 \pm 2.97$%, NIM-SE-SSNEDDS $= 77.76 \pm 4.29$%) and excellent flow properties. XRD analysis revealed drug amorphization as the characteristic diffraction peaks were absent; this offers a great advantage in improvement of drug dissolution.

SEM images revealed smoothening and filling of adsorbent surfaces by adsorbate. For NIM-SD-SSNEDDS, the size was 10–15 μm, and for NIM-SE-SSNEDDS, it was 20–25 μm. The SEM images provide visual evidence of the effective adsorption behaviour of microparticles, validating the excellent adsorption of liquid SNEDDS for both SD-CHEM and SE-CHEM.

FTIR confirmed no interaction of drug and excipients with the broadening of some characteristic drug peaks in the solid formulations because of the hydrogen bonding with surfactants. DSC analysis also confirmed the amorphization of the drug with the disappearance of the characteristic crystalline peaks of NIM.

Stability assessments confirmed the physical and thermodynamic robustness of reconstituted nanoemulsions, considering parameters such as droplet size, polydispersity index (PDI), zeta potential, emulsification time, per cent transmittance, and cloud temperature. For NIM-SD-SSNEDDS, these values were observed as follows: droplet size of 247.1 nm, PDI of 0.620, zeta potential of 1.353 mV, emulsification time ranging from 38 to 41 s,

Table 3 Stability data of the NIM-SD-SSNEDDS and NIM-SE-SSNEDDS

Formulation	Test parameters	Initial	1 month (40 ± 2 °C/75 ± 5% RH)	3 months (40 ± 2 °C/75 ± 5% RH)	6 months (40 ± 2 °C/75 ± 5% RH)
NIM-SD-SSNEDDS	Description	Yellow opaque capsules with SSNEDDS (No change in appearance)	Yellow opaque capsules with SSNEDDS (No change in appearance)	Yellow opaque capsules with SSNEDDS (No change in appearance)	Yellow opaque capsules with SSNEDDS (No change in appearance)
	%CDR	84.43% ± 1.3	83.08% ± 2.1	83.88% ± 1.7	82.59% ± 0.9
	Disintegration time (min.)	6 ± 0.3	6 ± 0.8	7 ± 1.4	7 ± 0.9
NIM-SE-SSNEDDS	Description	Yellow opaque capsules with SSNEDDS (No change in appearance)	Yellow opaque capsules with SSNEDDS (No change in appearance)	Yellow opaque capsules with SSNEDDS (No change in appearance)	Yellow opaque capsules with SSNEDDS (No change in appearance)
	%CDR	76.68% ± 2.3	76.43% ± 2.5	75.94% ± 1.4	75.13% ± 1.8
	Disintegration time (min.)	7 ± 0.5	7 ± 1.1	7 ± 0.8	8 ± 0.6

% CDR percentage of cumulative drug release, values are presented as mean ± standard deviation (S.D.), ($n = 3$)

per cent transmittance of 94.64%, and a cloud temperature of 54 °C. On the other hand, for NIM-SE-SSNEDDS, the corresponding values were 399.6 nm, PDI 0.821, zeta potential 1.351 mV, emulsification time ranging from 40 to 48 s, per cent transmittance of 92.96%, and a cloud temperature of 49 °C. These findings suggest that solid SNEDDS closely resemble liquid SNEDDS, indicating the stability of the reconstituted nanoemulsion.

FE-SEM images displayed the formation of droplets characterized by small sizes, with no observable evidence of coalescence, suggesting the stability of the reconstituted nanoemulsions. In vitro dissolution studies indicated a notable fourfold enhancement in drug dissolution for NIM-SD-SSNEDDS (84.43%) and NIM-SE-SSNEDDS (76.68%) when contrasted with the pure drug (28%). The ultimate drug release from liquid SNEDDS and solid SNEDDS exhibited similar patterns, demonstrating comparable release profiles. Ex vivo permeation studies revealed nearly identical profiles for NIM-SD-SSNEDDS (22.61%) and NIM-SE-SSNEDDS (21.93%) when compared to NIM-SNEDDS (25.02%). Stability study of both NIM-SD-SSNEDDS and NIM-SE-SSNEDDS confirmed that the preparations were stable for six months of accelerated stability study. Notably, NIM-SD-SSNEDDS demonstrated superior performance compared to NIM-SE-SSNEDDS, emphasizing the effectiveness of microparticles developed through the spray drying method (SD-CHEM) as adsorbents for solidification. These findings suggest that NIM-SD-SSNEDDS and NIM-SE-SSNEDDS can generate nanosized droplets in nanoemulsion containing the drug, facilitating successful drug diffusion across the biological membrane. These findings indicate improved dissolution and permeation for nimodipine in both solid SNEDDS formulations.

Conclusion

This study aimed to develop effective solid self-nanoemulsifying drug delivery systems (SNEDDS) for nimodipine with Cremophor RH 40, Lipoxol 300, and PEG 400 as the oil, surfactant, and co-surfactant. SNEDDS was formulated with an oil to Smix (surfactant/co-surfactant) ratio of 40:60, determined through a ternary phase diagram. Solid SNEDDS were created using previously developed microparticles (SD-CHEM and SE-CHEM) as adsorbents for NIM-SD-SSNEDDS and NIM-SE-SSNEDDS, respectively, with NIM-SNEDDS as an adsorbate for both. The final adsorbate (liquid NIM-SNEDDS): adsorbent ratio for NIM-SD-SSNEDDS and NIM-SE-SSNEDDS was 1:2.5. Both formulations exhibited favourable drug loading and flow properties. XRD analysis confirmed drug amorphization in both formulations, and SEM images verified uniform adsorption of liquid SNEDDS over solid microparticles. FTIR analysis indicated no interactions between excipients, while DSC analysis revealed the amorphous form of the drug in both solid SNEDDS. Both formulations showed nanometric globule sizes with minimal polydispersity indices. Stability studies and FE-SEM images confirmed reconstituted nanoemulsions' physical and thermodynamic stability. In vitro dissolution studies demonstrated nearly a fourfold increase in drug dissolution compared to pure drug. Both in vitro and ex vivo permeation studies revealed similar dissolution and permeation profiles for NIM-SD-SSNEDDS and NIM-SE-SSNEDDS compared to NIM-SNEDDS. Notably, NIM-SD-SSNEDDS outperformed NIM-SE-SSNEDDS, indicating the superior performance of microparticles developed by the spray drying method (SD-CHEM) as adsorbents for solidification. Enhanced dissolution and permeation for nimodipine in solid

Kumar *et al. Future Journal of Pharmaceutical Sciences*   (2024) 10:87

Page 16 of 17

SNEDDS were achieved. Both the formulation systems have proved their efficacy as S-SNEDDS, and the chitosan EDTA microparticle developed by spray drying and solvent evaporation can be utilized in future studies of different drugs SNEDDS to fabricate solid SNEDDS.

Abbreviations

NIM	Nimodipine
BCS	Biopharmaceutical classification system
SNEDDS	Self-nanoemulsifying drug delivery system
GIT	Gastrointestinal tract
S-SNEDDS	Solid self-nanoemulsifying drug delivery systems
NIM-SNEDDS	Liquid self-nanoemulsifying drug delivery system of the nimodipine
SD-CHEM	Spray-dried chitosan-EDTA microparticles
SE-CHEM	Solvent-evaporated chitosan-EDTA microparticles
S-SNEDDS	Solid self-nanoemulsifying drug delivery system
NIM-SD-SSNEDDS	Nimodipine solid self-nanoemulsifying drug delivery system with spray-dried microparticles
NIM-SE-SSNEDDS	Nimodipine solid self-nanoemulsifying drug delivery system with solvent-evaporated microparticles
XRD	X-ray diffraction
SEM	Scanning electron microscopy
FTIR	Fourier-transform infrared spectroscopy analysis
DSC	Differential scanning calorimetry
FE-SEM	Field emission scanning electron microscopy
PDI	Polydispersibility index
%CDR	% Cumulative drug release

Supplementary Information

The online version contains supplementary material available at https://doi.org/10.1186/s43094-024-00653-x.

Supplementary Material 1.

Declarations

Ethical approval and consent of participate
None.

Consent for publication
None.

Competing interests
The authors declare that they have no competing interests.

Author details
[1]Department of Pharmaceutical Sciences, HNB Garhwal (A Central) University, Srinagar, Garhwal, Uttarakhand, India. [2]University Institute of Pharmaceutical Sciences and Research, Baba Farid University of Health Sciences, Faridkot, Punjab, India.

References

1. Zhu Y, Ye J, Zhang Q (2020) Self-emulsifying drug delivery system improve oral bioavailability: role of excipients and physico-chemical characterization. PNT 8:290–301
2. Mhango EKG, Sveinbjornsson BR, Snorradottir BS, Gizurarson S (2024) Incompatibility of antimalarial drugs: challenges in formulating combination products for malaria. Drug Deliv 31:2299594
3. Tekeli MC, Aktas Y, Celebi N (2021) Oral self-nanoemulsifying formulation of GLP-1 agonist peptide exendin-4: development, characterization and permeability assesment on Caco-2 cell monolayer. Amino Acids 53:73–88
4. Truong DH, Tran TH, Ramasamy T, Choi JY, Lee HH, Moon C, Choi H-G, Yong CS, Kim JO (2016) Development of solid self-emulsifying formulation for improving the oral bioavailability of erlotinib. AAPS PharmSciTech 17:466–473
5. Yang X, Li W, Li S et al (2024) Fish oil-based microemulsion can efficiently deliver oral peptide blocking PD-1/PD-L1 and simultaneously induce ferroptosis for cancer immunotherapy. J Control Release 365:654–667
6. Friedl JD, Jörgensen AM, Le-Vinh B, Braun DE, Tribus M, Bernkop-Schnürch A (2021) Solidification of self-emulsifying drug delivery systems (SEDDS): impact on storage stability of a therapeutic protein. J Colloid Interface Sci 584:684–697
7. Yi T, Wan J, Xu H, Yang X (2008) Controlled poorly soluble drug release from solid self-microemulsifying formulations with high viscosity hydroxypropylmethylcellulose. Eur J Pharm Sci 34:274–280
8. Seo YG, Kim D-W, Cho KH, Yousaf AM, Kim DS, Kim JH, Kim JO, Yong CS, Choi H-G (2015) Preparation and pharmaceutical evaluation of new tacrolimus-loaded solid self-emulsifying drug delivery system. Arch Pharm Res 38:223–228
9. Savjani KT, Gajjar AK, Savjani JK (2012) Drug solubility: importance and enhancement techniques. ISRN Pharm 2012:1–10
10. Kumar M, Chawla PA, Faruk A, Chawla V (2023) Spray drying as an effective method in the development of solid self- emulsifying drug delivery systems. Curr Drug Deliv 20:508–525
11. Teng Z, Yu M, Ding Y, Zhang H, Shen Y, Jiang M, Liu P, Opoku-Damoah Y, Webster TJ, Zhou J (2018) Preparation and characterization of nimodipine-loaded nanostructured lipid systems for enhanced solubility and bioavailability. IJN 14:119–133
12. Wessell A, Kole MJ, Badjatia N, Parikh G, Albrecht JS, Schreibman DL, Simard JM (2017) High compliance with scheduled nimodipine is associated with better outcome in aneurysmal subarachnoid hemorrhage patients cotreated with heparin infusion. Front Neurol 8:268
13. Vergouwen MD, Vermeulen M, Roos YB (2006) Effect of nimodipine on outcome in patients with traumatic subarachnoid haemorrhage: a systematic review. Lancet Neurol 5:1029–1032
14. Yi T, Wan J, Xu H, Yang X (2008) A new solid self-microemulsifying formulation prepared by spray-drying to improve the oral bioavailability of poorly water soluble drugs. Eur J Pharm Biopharm 70:439–444
15. Liu Y, Qiu H-C, Su J, Jiang W-J (2016) Drug treatment of cerebral vasospasm after subarachnoid hemorrhage following aneurysms. Chin Neurosurg J 2:4
16. Kale AA, Patravale VB (2008) Design and evaluation of self-emulsifying drug delivery systems (SEDDS) of nimodipine. AAPS PharmSciTech 9:191–196
17. Huang Y, Zhang S, Shen H, Li J, Gao C (2018) Controlled release of the nimodipine-loaded self-microemulsion osmotic pump capsules: development and characterization. AAPS PharmSciTech 19:1308–1319
18. Sin JH, Shafeeq H, Levy ZD (2018) Nimodipine for the treatment of otolaryngic indications. Am J Health Syst Pharm 75:1369–1377
19. AlSheyyab RY, Obaidat RM, Altall YR, Abuhuwaij RT, Ghanma RR, Ailabouni AS, Mashaqbeh HA, Al-Haj S (2019) Solubility enhancement of nimodipine through preparation of Soluplus® dispersions. J Appl Pharm Sci 9:030–037

20. Yi T, Zhang J (2019) Effects of hydrophilic carriers on structural transitions and in vitro properties of solid self-microemulsifying drug delivery systems. Pharmaceutics 11:267

21. Sirvi A, Kuche K, Chaudhari D, Ghadi R, Date T, Katiyar SS, Jain S (2022) Supersaturable self-emulsifying drug delivery system: a strategy for improving the loading and oral bioavailability of quercetin. J Drug Deliv Sci Technol 71:103289

22. ElShagea HN, ElKasabgy NA, Fahmy RH, Basalious EB (2019) Freeze-dried self-nanoemulsifying self-nanosuspension (SNESNS): a new approach for the preparation of a highly drug-loaded dosage form. AAPS PharmSciTech 20:258

23. Verma R, Mittal V, Kaushik D (2018) Quality based design approach for improving oral bioavailability of valsartan loaded SMEDDS and study of impact of lipolysis on the drug diffusion. DDL 8:130–139

24. Lee J-H, Kim H, Cho Y, Koo T-S, Lee G (2018) Development and evaluation of raloxifene-hydrochloride-loaded supersaturatable SMEDDS containing an acidifier. Pharmaceutics 10:78

25. Verma R, Kaushik D (2020) Design and optimization of candesartan loaded self-nanoemulsifying drug delivery system for improving its dissolution rate and pharmacodynamic potential. Drug Deliv 27:756–771

26. Mohd AB, Sanka K, Bandi S, Diwan PV, Shastri N (2015) Solid self-nanoemulsifying drug delivery system (S-SNEDDS) for oral delivery of glimepiride: development and antidiabetic activity in albino rabbits. Drug Deliv 22:499–508

27. Kumar M, Chawla PA, Faruk A, Chawla V, Thakur S, Jain SK (2024) Development of superior chitosan–EDTA microparticles as an adsorbent base for solidifying the self-emulsifying drug delivery systems. Future J Pharm Sci 10:18

28. Verma S, Singh SK, Verma PRP (2016) Solidified SNEDDS of loratadine: formulation using hydrophilic and hydrophobic grades of Aerosil®, pharmacokinetic evaluations and in vivo–in silico predictions using GastroPlus™. RSC Adv 6:3099–3116

29. Dixit M, Kini AG, Kulkarni PK (2010) Preparation and characterization of microparticles of piroxicam by spray drying and spray chilling methods. Res Pharm Sci 5:89–97

30. Shazly G, Mohsin K (2015) Dissolution improvement of solid self-emulsifying drug delivery systems of fenofi brate using an inorganic high surface adsorption material. Acta Pharm 65:29–42

31. Blindheim FH, Ruwoldt J (2023) The effect of sample preparation techniques on lignin Fourier transform infrared spectroscopy. Polymers 15:2901

32. Bang SP, Yeon CY, Adhikari N, Neupane S, Kim H, Lee DC, Son MJ, Lee HG, Kim J-Y, Jun JH (2019) Cyclosporine A eyedrops with self-nanoemulsifying drug delivery systems have improved physicochemical properties and efficacy against dry eye disease in a murine dry eye model. PLoS ONE 14:e0224805

33. Rathore C, Hemrajani C, Sharma AK et al (2023) Self-nanoemulsifying drug delivery system (SNEDDS) mediated improved oral bioavailability of thymoquinone: optimization, characterization, pharmacokinetic, and hepatotoxicity studies. Drug Deliv Transl Res 13:292–307

34. Rangaraj N, Shah S, Maruthi AJ, Pailla SR, Cheruvu HS, Sampathi S (2019) Quality by design approach for the development of self-emulsifying systems for oral delivery of febuxostat: pharmacokinetic and pharmacodynamic evaluation. AAPS PharmSciTech 20:267

35. Beg S, Jena SS, Patra CN, Rizwan M, Swain S, Sruti J, Rao MEB, Singh B (2013) Development of solid self-nanoemulsifying granules (SSNEGs) of ondansetron hydrochloride with enhanced bioavailability potential. Colloids Surf B 101:414–423

36. Beg S, Katare OP, Saini S, Garg B, Khurana RK, Singh B (2016) Solid self-nanoemulsifying systems of olmesartan medoxomil: formulation development, micromeritic characterization, in vitro and in vivo evaluation. Powder Technol 294:93–104

37. Bandyopadhyay S, Katare OP, Singh B (2012) Optimized self nano-emulsifying systems of ezetimibe with enhanced bioavailability potential using long chain and medium chain triglycerides. Colloids Surf B 100:50–61

38. Janakiraman AK, Islam T, Liew KB, Elumalai M, Hanish Singh JC (2022) Improved oral bioavailability of poorly water-soluble vorinostat by self-microemulsifying drug delivery system. Beni-Suef Univ J Basic Appl Sci 11:99

39. Hussain A, Kumar Singh S, Ranjan Prasad Verma P, Singh N, Jalees Ahmad F (2017) Experimental design-based optimization of lipid nanocarrier as delivery system against *Mycobacterium* species: *in vitro* and *in vivo* evaluation. Pharm Dev Technol 22:910–927

40. Singh K, Tiwary AK, Rana V (2013) Spray dried chitosan–EDTA superior microparticles as solid substrate for the oral delivery of amphotericin B. Int J Biol Macromol 58:310–319

41. Mohd Izham MN, Hussin Y, Aziz MNM, Yeap SK, Rahman HS, Masarudin MJ, Mohamad NE, Abdullah R, Alitheen NB (2019) Preparation and characterization of self nano-emulsifying drug delivery system loaded with citraland its antiproliferative effect on colorectal cells in vitro. Nanomaterials 9:1028

42. Parmar N, Singla N, Amin S, Kohli K (2011) Study of cosurfactant effect on nanoemulsifying area and development of lercanidipine loaded (SNEDDS) self nanoemulsifying drug delivery system. Colloids Surf B 86:327–338

43. Qi X, Wang L, Zhu J, Hu Z, Zhang J (2011) Self-double-emulsifying drug delivery system (SDEDDS): a new way for oral delivery of drugs with high solubility and low permeability. Int J Pharm 409:245–251

44. Nepal PR, Han H-K, Choi H-K (2010) Preparation and in vitro–in vivo evaluation of Witepsol® H35 based self-nanoemulsifying drug delivery systems (SNEDDS) of coenzyme Q10. Eur J Pharm Sci 39:224–232

45. Balakumar K, Raghavan CV, Selvan NT, Prasad RH, Abdu S (2013) Self nanoemulsifying drug delivery system (SNEDDS) of Rosuvastatin calcium: design, formulation, bioavailability and pharmacokinetic evaluation. Colloids Surf B 112:337–343

46. Helmy SA, El-Bedaiwy HM, El-Masry SM (2020) Applying biopharmaceutical classification system criteria to predict the potential effect of Cremophor ® RH 40 on fexofenadine bioavailability at higher doses. Ther Deliv 11:447–464

47. Lukman Z, Anuar N, Abu Bakar NF, Abdul Rahman N (2020) Characterization and prediction of the non-bonded molecular interactions between racemic ibuprofen and α-lactose monohydrate crystals produced from melt granulation and slow evaporation crystallization. Indones J Chem 20:1255

48. Sahu M, Reddy VRM, Kim B, Patro B, Park C, Kim WK, Sharma P (2022) Fabrication of Cu_2ZnSnS_4 light absorber using a cost-effective mechano-chemical method for photovoltaic applications. Materials 15:1708

49. Semcheddine F, Guissi NEI, Liu X, Wu Z, Wang B (2015) Effects of the preparation method on the formation of true nimodipine SBE-β-CD/HP-β-CD inclusion complexes and their dissolution rates enhancement. AAPS PharmSciTech 16:704–715

50. Xu X, Chen X, Wang Z, Jing X (2009) Ultrafine PEG–PLA fibers loaded with both paclitaxel and doxorubicin hydrochloride and their in vitro cytotoxicity. Eur J Pharm Biopharm 72:18–25

51. Papageorgiou GZ, Bikiaris D, Karavas E, Politis S, Docoslis A, Park Y, Stergiou A, Georgarakis E (2006) Effect of physical state and particle size distribution on dissolution enhancement of nimodipine/PEG solid dispersions prepared by melt mixing and solvent evaporation. AAPS J 8:E623–E631

52. Alwadei M, Kazi M, Alanazi FK (2019) Novel oral dosage regimen based on self-nanoemulsifying drug delivery systems for codelivery of phytochemicals: curcumin and thymoquinone. Saudi Pharm J 27:866–876

53. Choi K-O, Aditya NP, Ko S (2014) Effect of aqueous pH and electrolyte concentration on structure, stability and flow behavior of non-ionic surfactant based solid lipid nanoparticles. Food Chem 147:239–244

54. Baviskar PS, Mahajan HS, Chandankar SM, Agrawal YO (2022) Development and evaluation of N-acetyl glucosamine-decorated vitamin-E-based micelles incorporating resveratrol for cancer therapy. J Drug Deliv Sci Technol 78:103965

Publisher's Note